Iranian Journal of Electrical and Electronic Engineering

Journal Homepage: ijeee.iust.ac.ir

Research Paper

Real-Time Discrimination of Symmetrical Faults from Power Swings

H. Yaghobi*(C.A.)

Abstract: For reliable operation, distance relays have to be blocked in case of stable power swings (SPSs). Because these relays are prone to detect an SPS as a symmetrical 3-phase fault according to their symmetric nature. It should be noted that there are zero and negative sequence components during asymmetrical faults. However, these components do not exist during stable fluctuations or symmetrical faults. Consequently, according to the symmetric nature of the stable fluctuation, the distance relay may experience maloperation. This article proposes a new technique to discriminate a symmetrical 3-phase fault from an SPS. The proposed technique is based on the extraction of the exponentially decaying DC component in the 3-phase current by using the MIMIC impedance. This technique can detect the symmetrical fault in less than a quarter of one power cycle. The suitability of the technique is shown by simulating various symmetrical faults during fast and slow SPS conditions.

Keywords: Maloperation of Distance Relay, Mimic Impedance, Power swings, Symmetrical Faults.

1 Introduction

THE analysis of the North American power swings that happened on August 14, 2003, has implied that power swing is one of the serious conditions that caused the undesired trip of distance relays and finally resulted in a power network blackout [1]-[4]. It is worth highlighting that the distance relays are prone to detect a stable fluctuation as a symmetrical 3-phase fault. Consequently, these relays are blocked during the stable fluctuation to avoid an unwanted operation. However, if a symmetrical 3-phase fault happens during a stable fluctuation, it should be detected as soon as possible [5]. There are zero and negative sequence components during asymmetrical faults.

Iranian Journal of Electrical and Electronic Engineering, 2023.
Paper first received 12 Sep 2022, revised 18 Apr 2023, and accepted 26 Apr 2023.
*The author is with Faculty of Electrical and Computer Engineering, Semnan University, Semnan, Iran.
E-mails: yaghobi@semnan.ac.ir.
Corresponding Author: H. Yaghobi.
https://doi.org/10.22068/IJEEE.19.2.2658.

With the presence of these components, it is easily possible to discriminate an asymmetrical fault from a stable fluctuation. On the other hand, these components do not exist during stable fluctuations or symmetrical faults. Therefore, according to the symmetric nature of the stable fluctuation, discrimination of symmetrical faults from stable fluctuation is an important issue and the distance relay may experience maloperation in this condition [5].

Different fault detection techniques have been proposed in the literature to detect symmetrical 3-phase faults during stable power fluctuation. Most of the techniques in this field are based on using the rate of change of a particular parameter during power swing detection. The popular and commonly used techniques for distinguishing a stable fluctuation are to measure the rate of change of positive sequence impedance as they use the blinders and a timer in the R–X plane [6].

Such techniques need deliberate time delay to prevent probable misoperation. However, this

deliberate time delay is not a perfect solution. Because in real cases of fault situations, the intentional time delay increases the stress on the network or misoperation of the other relays.

The rate of variation of swing center voltage (SCV) to detect power swings was proposed by the reference [7]. The technique presented in [8], [9], uses the rate of change in the voltage phase angle to distinguish faults occurring during power swings. In these references, 3-phase symmetrical faults have not been considered, and only single-phase fault has been applied.

The rate of variation of 3-phase powers has been introduced in [10] for detecting faults. The method presented in [11], uses the rate of variation of resistance to detect symmetrical faults. Reference [12] proposed the rate of variation of the FFT coefficients of the fundamental frequency component of the active power to discriminate 3-phase symmetrical faults occurring during power swings. Furthermore, in reference [13] a technique based on the decaying DC component of fault currents has been suggested to discriminate a symmetrical fault from a power swing. In the proposed technique, the DC component of the current waveform is obtained from FFT analysis. However, it should be noted that the Fourier transform only finds the constant DC component and is not able to find the exponentially decaying DC component [14].

On the other hand, the general disadvantage of these approaches, which use the rate of change of a particular parameter, is that they depend on the frequency of the power swings. Reference [15] proposed a technique based on the extraction of the DC component of the 3-phase currents utilizing the Prony method. Furthermore, reference [16] proposed a method that uses the local current. The method is based on the fact that during a power fluctuation, the 3-phase current is subjected to amplitude modulation, while during a symmetrical 3-phase fault if its DC component is completely removed, the current waveform resembles an AC sinusoidal waveform. In this condition, by completely removing the DC component, the rate of variation of the current amplitude phasor becomes zero, whereas it will be non-zero during swing time intervals. However, the complete elimination of the DC component is mandatory in this method.

In [17], a new method using the positive sequence current data of two ends of the transmission line has been proposed. However, communication channels, some phasor measurement units (PMUs), and data synchronization are needed in this method. In order to improve fault detection during the power swing, some techniques based on Taylor Series expansion are developed in [18], [19]. It should be noted that these techniques may fail to prevent the misoperation of the distance relay during voltage instability situations and load encroachment [20]. Reference [21] introduced a method by using a special wave pattern in the negative sequence phasor to detect power swings from faults.

In [22], the technique based on the wavelet transform (WT) has been presented. In general, WT-based techniques are vulnerable to noise. Some other intelligent-based techniques are also presented in [23], for discriminating the 3-phase symmetrical faults occurring during power swings. However, these techniques depend on the power network structure and require a large amount of data for the training of all probable conditions [24].

During a power swing, the probability of power system instability is higher. Therefore, the simplicity and speed of the fault detector are very important in diagnosis. Consequently, this article proposes a very fast symmetrical fault detector for use in distance relays. The technique is able to detect the symmetrical fault in less than a quarter of one power cycle. This detector is based on the extraction of the exponentially decaying DC component in the 3-phase current by using the MIMIC filter. It is noteworthy that it has been proven in the authentic references [15], [25] that when a fault occurs, an exponentially decaying DC component appears in the current waveform, while this decaying DC component does not exist in power swing conditions.

It should be noted that the technique presented in the authentic reference [15] has been modified by using the MIMIC filter. In [15], the Prony method is used to extract the exponentially decaying DC component in the 3-phase current, while in this research, the MIMIC filter is used for this purpose. It is worth highlighting that the MIMIC filter has long been used in some commercial relays in operational conditions [26]. However, the Prony method was not operationally studied in different practical conditions. In other words, the performance of the MIMIC filter has been confirmed in practical application. On the other hand, because this filter is available in some digital relays, there is no need to add a new program in terms of processing speed and memory size. Another point worth highlighting is that in order to completely remove the DC component by the MIMIC filter, the time constant of this filter must be close to the time constant of the

fault. However, to discriminate a symmetrical 3-phase fault from a stable power swing, it is not necessary to completely remove the DC component. In fact, only the presence of the DC component in the waveform indicates a symmetrical 3-phase fault has happened.

It is noteworthy that in the discussion of stable power swings, there are other issues such as detecting unstable power swings and asymmetrical faults. However, this study only considers symmetrical faults as the main concern in this field. In fact, the proposed method can be added as an auxiliary function to existing methods that succeed in detecting unstable power swings and asymmetrical faults [5], [27]-[29]. For example, negative/zero component-based techniques are powerful in asymmetrical conditions. But, these methods do not work well in the event of symmetrical faults. With the presence of negative/zero components during asymmetrical faults, it is easily possible to discriminate an asymmetrical fault from an SPS. Conversely, these components do not exist during SPS or symmetrical faults. The merit of the proposed technique is shown by simulating various symmetrical faults during fast and slow stable power swing conditions. The results demonstrate that this detector can be easily implemented in digital relays and severely increases the accuracy and sensitivity of distance protection. Finally, it should be noted that the methods which are based on the extraction of the DC component from transient signals are vulnerable to external faults (i.e. the fault in a transmission line where the relay is not installed) because both internal and external faults produce an exponentially decaying DC component in the current waveform.

2 Mimic Impedance

Power networks are typically inductive in nature. As shown in Fig. 1, if the shunt capacitances are ignored, the power network can be modeled as a series R-L circuit. If a fault occurs in the power network, an exponentially decaying DC component appears in the current waveform as follows [25]:

$$I(t) = I_m \sin(wt + \alpha - \phi) + I_m \sin(\alpha - \phi) e^{-t/\tau},$$
$$I_m = \frac{V_m}{Z},\ Z^2 = R^2 + X^2,\ \tau = \frac{L}{R},\ \phi = \tan^{-1}\left(\frac{wL}{R}\right) \quad (1)$$

where α is the fault inception angle. In the current equation, the first term is the steady-state fault current and the second term is the exponentially decaying DC component. The DC component is important in high-speed relays. Because this component becomes insignificant after approximately 5-time constants after the fault occurs.

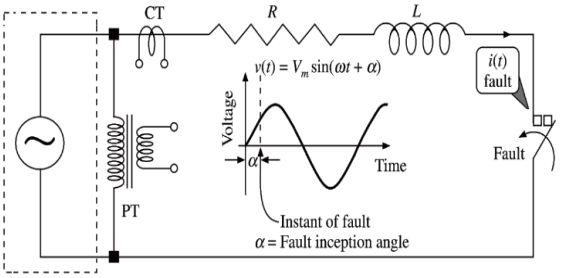

Fig. 1 Power network feeding into fault [25].

By using the MIMIC impedance in the secondary circuit of the current transformer (with the same L/R ratio as the primary power circuit), the decaying DC component can be successfully eliminated. As shown in Fig. 2, the voltage through the MIMIC impedance can be found as follows [25]:

$$v(t) = KRi(t) + KLdi(t)/dt \quad (2)$$

Substituting the exponentially decaying DC component $I_m e^{-t/\tau}$, $\tau = L/R$ and derivation yields [22]:

$$v_{mimic} = KRI_m e^{-t/\tau} - KLI_m \frac{1}{\tau} e^{-t/\tau} = 0 \quad (3)$$

Therefore, the use of MIMIC impedance entirely removes the exponentially decaying DC component.

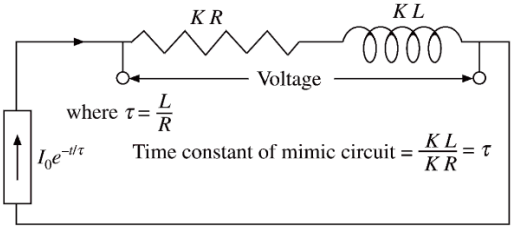

Fig. 2 Response of mimic impedance to exponentially decaying DC component [25].

However, it should be noted that this entire elimination was possible because the MIMIC impedance parameters were exactly equal to the decaying DC current time constant. This condition is not always probable and may lead to imperfect elimination of the decaying DC component. It is worth highlighting that this incomplete elimination is not important in the method proposed in this paper, which will be described in the next section.

3 Proposed Algorithm Based on the Real-time Digital MIMIC Impedance

Since the suggested technique is based on the real-time discrimination of symmetrical faults from

stable power swing by using MIMIC Impedance, this section is dedicated to reaching an appropriate technique for extraction of the exponentially decaying DC component in the 3-phase current by using the digital MIMIC filter. As stated earlier, when a fault occurs, an exponentially decaying DC component appears in the current waveform, while this decaying DC component does not exist in power swing conditions. Equation (2) can be discretized as follows:

$$v(t_n) = KRi(t_n) + KL\left(\frac{i(t_n) - \mathrm{i}(t_{n-1})}{\Delta t}\right) \quad (4)$$

where *n* is the number of each sample. Taking the Z-transform of the Eq. (4) yields:

$$v(z) = KRI(z) + \frac{KL}{\Delta t}\left(I(z) - Z^{-1}I(z)\right) \quad (5)$$

By substituting $\tau = L/R$ and doing some manipulations, (5) can be written as follows:

$$v(z) = KR\left(I(z) + \frac{\tau I(z)}{\Delta t}[1 - Z^{-1}]\right) \quad (6)$$

By representing $\tau/\Delta t = \tau_1$, Eq. (6) can be expressed as:

$$\frac{v(z)}{I(z)} = H(z) = KR\left[(1+\tau_1) - \tau_1 Z^{-1}\right] \quad (7)$$

where $K_m = KR$ is the gain term. This gain term is set so that the filter gain will be equal to one at the rated frequency (i.e. 50 or 60 Hz). At 60 Hz rated frequency, substituting $Z = e^{jwT} = e^{j2\pi 60T}$ and $T = 1/f_s$, yields:

$$K_m\left[(1+\tau_1) - \tau_1 e^{-j2\pi 60/f_s}\right] = 1 \quad (8)$$

where f_s is the sampling frequency. By doing some manipulations, Eq. (8) can be found as below:

$$K_m = \frac{1}{\sqrt{\left[(1+\tau_1) - \tau_1\cos(\frac{2\pi 60}{f_s})\right]^2 + \left[\tau_1 \sin(\frac{2\pi 60}{f_s})\right]^2}} \quad (9)$$

On the other hand, as stated earlier, when a fault occurs, an exponentially decaying DC component appears in the current waveform. Consequently, the fault current can be found as below:

$$I(t) = I_0 e^{-t/\tau} + \sum_{m=1}^{\frac{N}{2}-1} I_m \sin(mw_1 t + \phi_m) \quad (10)$$

where I_0 is the DC offset amplitude, I_m is the m-th AC component magnitude and ϕ_m is m-th AC component initial angle. This current by uniformly sampling each ΔT can be expressed as follows:

$$I_k = I_0 r^k + \sum_{m=1}^{\frac{N}{2}-1} I_m \sin(\frac{2\pi k}{N} m + \phi_m),\ k = 0,1,.....N, \quad (11)$$

$$r = e^{-(\Delta T/\tau)}$$

If this current waveform comprises a decaying DC component, a symmetrical 3-phase fault has happened, otherwise a stable power swing has occurred. In the other words, the presence of the exponentially decaying DC part in an unknown current can be utilized as an indicator for detecting the symmetrical fault. The magnitude of the DC component and its time constant varies depending on the location, instant, and the resistance of the fault. However, it is worth highlighting that the proposed method does not need to accurately calculate the time constant of the DC component, and is based only on the presence of the DC component.

As stated earlier, it should be noted that in order to completely remove the DC component by the MIMIC filter, the time constant of this filter must be close to the time constant of the fault. However, to discriminate a symmetrical 3-phase fault from a stable power swing, it is not necessary to completely remove the DC component. In fact, only the presence of the DC component in the waveform indicates a symmetrical 3-phase fault has happened. Therefore, the time constant of the exponentially decaying DC component can be approximated.

On the other hand, it should be noted that the primary time constant in the power system for transmission lines is approximately 16.67 ms for a 60 Hz power network ($1/60 = 16.67$ ms) [30]. Furthermore, it is well known that the decaying DC term will become insignificant after a time equal 5-time constants after the instant of disturbance. Therefore 5-time constants will be approximately equal to 84 ms at a frequency of 60 Hz ($5 \times 16.67 \approx 84$ ms).

It is worth highlighting that this time constant can be accurately calculated by the two methods presented in [31]. The presented methods in [31] utilize four sampled data by half and full-cycle algorithms as shown in Fig. 3. This time constant can be obtained in half and full-cycle algorithms by Eq. (12) and Eq. (13), respectively. It is clear that if Eqs. (12) and (13) are used to calculate the time constant, the detection time by the proposed algorithm in this research will be longer.

$$\tau = \frac{1}{f_s \ln\frac{x(1) + x(N/2+1)}{x(2) + x(N/2+2)}} \quad (12)$$

$$\tau = \frac{1}{f_s \ln\frac{x(1) - x(N+1)}{x(2) - x(N+2)}} \quad (13)$$

where f_s is the sampling frequency. Fig. 4 illustrates the flowchart of the suggested technique.

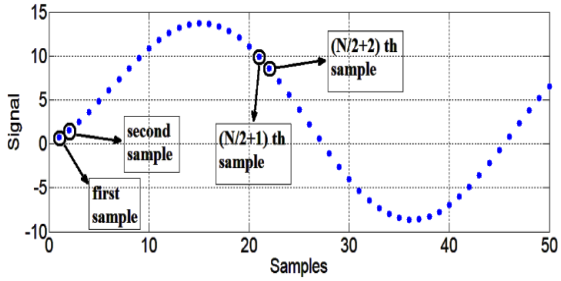

(a)

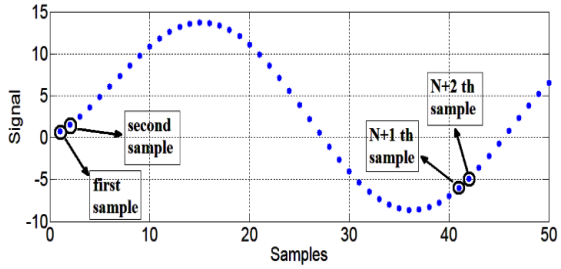

(b)

Fig. 3 Four sampled data to calculate time constant [30]. (a) Half cycle algorithm. (b) Full cycle algorithm.

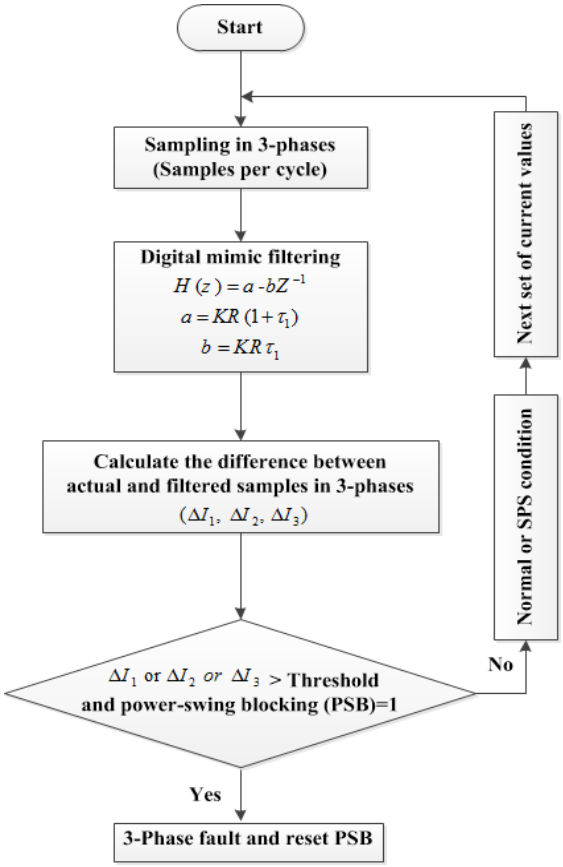

Fig. 4 Flowchart of the proposed detection technique.

Firstly, the unknown current waveform is sampled at an arbitrary sampling rate, and the first set of discrete current values $\{I_0, I_1, ..., I_N\}$ processes for extraction of the exponentially decaying DC component by using the digital MIMIC filter represented by Eq. (7). It is noteworthy that the coefficients of the digital MIMIC filter for various sampling rates are presented in Table 1. Then, the differential current ΔI is computed from the difference in filtered and genuine samples of current. This differential current is insignificant for stable power swings, and it is substantial during 3-phase symmetrical faults. Thus, the suggested flowchart detects the fault situation if the differential current ΔI exceeds the threshold value.

Table 1 Coefficients of digital MIMIC filter for different sampling rate

Samples per cycle	Digital MIMIC filter
12	1.9411-1.9219 Z^{-1}
16	2.5748-2.5494 Z^{-1}
24	3.8469-3.8088 Z^{-1}
32	5.1199-5.0693 Z^{-1}
64	10.1886-10.0877 Z^{-1}
128	20.0672-19.8686 Z^{-1}
256	37.9477-37.5720 Z^{-1}

It is worth highlighting that this threshold value is intended in the flowchart for consideration of the contamination of noise and other dynamic oscillations. After installing the relay in the power system, it is possible to use the analysis of practical data in a limited period of time to determine a suitable threshold value in the proposed method. In fact, as stated earlier, the value of this threshold depends on the noises and dynamic oscillations of the desired network. So, first, an initial value for the threshold can be set in the relay. Then, after installing the digital relay in the desired network, this initial value can be corrected by analyzing practical data in a limited period of time.

Another point worth highlighting is that during normal conditions, such as SPS conditions, there is a small value of the DC component. It should be noted that in these conditions or transient disturbances that are not harmful to the power system, the protection system should not trip. It should be noted that to discriminate an asymmetrical fault from a stable fluctuation, the proposed technique needs an auxiliary function based on negative/zero components.

Typical behavior of the original and filtered signals during a power swing and 3-phase symmetrical fault are shown in Fig. 5. Furthermore, for better illustration, the amplitude of the differential decaying DC component (i.e. ΔI - the difference between filtered and genuine samples of current) during these conditions are presented in Fig. 6.

According to Fig. 6, a 3-phase symmetrical fault current contains decaying DC components. However, there are no such components in the

current waveform following a power swing. In these cases, a digital mimic filter with 64 samples per cycle at the fundamental frequency is used. It should be noted that the average value of the differential current samples (AVDCS) in a quarter of one power cycle for the power swing and 3-phase symmetrical fault is 0.015 and 1.003 p.u., respectively. Consequently, as stated earlier, the presence of the exponentially decaying DC part of an unknown current can be utilized as an indicator for detecting the symmetrical fault.

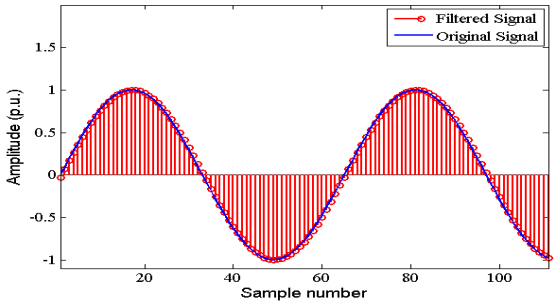

(a)

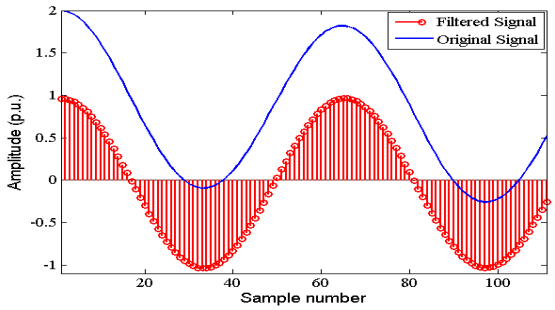

(b)

Fig. 5 Typical behavior of the original and filtered signals (a) Following a power swing, (b) Following a 3-phase symmetrical fault

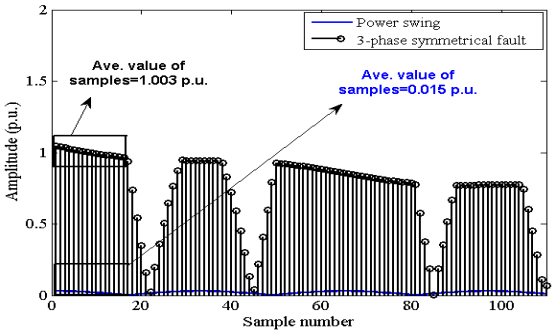

Fig. 6 Amplitude of the differential decaying DC component (i.e. difference between filtered and genuine samples of current) during a power swing and 3-phase symmetrical fault

4 Performances of the Proposed Technique

To demonstrate the suitability of the proposed technique, two power networks shown in Fig. 7, one of which is compensated by a series capacitor, are modeled using the "Matlab/Simulink" software. Details of the power networks are given in [32], [33]. In these power networks, a machine rated 600 MVA, 22 kV, 60 Hz, 3600 rpm with an excitation system, steam turbine, and power system stabilizer (PSS) have been used.

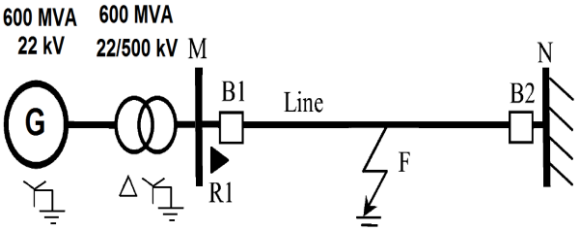

(a)

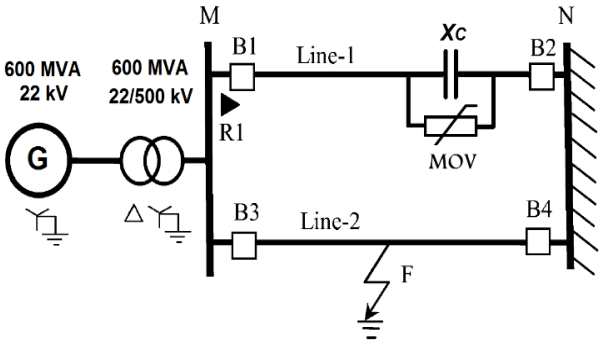

(b)

Fig. 7 Simulated power network. (a) 500 kV line transmission network. (b) 500 kV IEEE benchmark model for series-compensated network.

Power swing conditions can be produced due to a disturbance such as generator tripping, load shedding, line switching, short-circuit faults, etc. [34], [35]. On the other hand, it is noteworthy that the magnitude and time constant of the exponentially decaying DC component is unknown and depend on the fault location, fault inception time, and fault resistance [15], [17]. Consequently, to show this behavior, various test scenarios are conducted by varying fault resistance, fault inception time, fault inception angle, and fault location. In other words, the impact of these parameters was investigated and in all different test scenarios, the selectivity of the suggested technique was proven. The results of the performances of the suggested technique are summarized in Tables 2 and 3.

4.1 Single-circuit Line

To illustrate the usefulness of the proposed technique, a 500-kV power network with a single line as illustrated in Fig. 7 (a) is used. As stated earlier, various test scenarios are generated by varying fault location, fault resistance, fault inception time, and fault inception angle.

Table 2 Different cases for studying the performance of suggested technique

Case	Fault location (Km)	Fault Inception (s)	Fault Inception Angle (deg.)	Fault Resistance (ohm)	Average of the differential current samples (ΔI) in quarter of one cycle (p.u.)	
					Symmetrical fault conditions	Power swing conditions
1	10	1	0	5	1.7504	0.052
2	20	1.00138	25	5	1.7202	0.045
3	30	1.00277	50	4	1.4201	0.0251
4	35	1.004166	75	4	1.6502	0.0321
5	40	1.005	90	3	1.7209	0.0391
6	50	1	0	3	1.4682	0.036
7	60	1.00138	25	2	1.4212	0.0323
8	70	1.00277	50	2	1.3802	0.0283
9	80	1.004166	75	1	1.6203	0.02902
10	90	1.005	90	1	1.6905	0.0311
11	95	1	0	0	1.2605	0.01137

Table 3 Different cases for studying the performance of suggested technique in the presence of series-compensated line

Case	Degree of Compensation (%)	Fault location (Km)	Fault Inception (s)	Fault Inception Angle (deg.)	Fault Resistance (ohm)	Average of the differential current samples (ΔI) in quarter of one cycle (p.u.)	
						Symmetrical fault conditions	Power swing conditions
12	25	10	1	0	5	1.3548	0.042
13	30	20	1.00138	25	5	1.7960	0.025
14	35	30	1.00277	50	4	1.8506	0.0312
15	40	35	1.004166	75	4	1.9608	0.0212
16	45	40	1.005	90	3	2.1504	0.0145
17	50	50	1	0	3	1.9021	0.006
18	55	60	1.00138	25	2	1.8096	0.0019
19	60	70	1.00277	50	2	1.7405	0.0282
20	65	80	1.004166	75	1	1.9408	0.0182
21	70	90	1.005	90	1	1.2.2405	0.0165
22	70	95	1	0	0	1.1945	0.0035

For creating the power swing condition in different cases, a temporary fault with various duration is applied after the beginning of the simulation.

For all the examined cases, the average value of the differential current samples (AVDCS) in a quarter of one power cycle for the power swing and 3-phase symmetrical fault is also calculated. These test scenarios and the associated results are presented in Table 2. According to Table 2, it can be clearly seen that AVDCS has negligible value during the power swing, whereas it has considerable value following a 3-phase symmetrical fault. During case 1, a symmetrical fault occurs at the 1st second with inception angle of 0°. In this case, fault resistance and fault location are considered 5 ohm and 10 km from the relay location, respectively. Fig. 8(a) shows the original and filtered signals following the power swing and 3-phase symmetrical fault. Furthermore, Fig. 8(b) shows the magnitude of the differential decaying DC components (i.e. ΔI) during these power swing and 3-phase symmetrical fault. As stated earlier and due to this figure, it can be clearly seen that during power swing conditions, the amount of the AVDCS is negligible value, whereas it increases to a considerable value after the fault inception.

In addition, to show the similarity in characteristics, Figs. 9 and 10 illustrate the original signal, filtered signals, and magnitude of the differential decaying DC component (i.e. ΔI) following a power swing and 3-phase symmetrical fault during cases 5 and 8. According to these Figs, it can be seen that the amplitude of the differential decaying DC component has a unique behavior in different test scenarios, and its general pattern is not affected by the fault resistance, fault inception time, and fault location.

4.2 Double-circuit Line with Compensation

One of the most common methods of compensation in a transmission line is the use of series capacitors. Compensation with series capacitors increases line capacity and reduces line losses. However, the presence of a series capacitor causes problems such as sub-synchronous resonance (SSR) and the effect of nonlinear impedance of its protection equipment during faults.

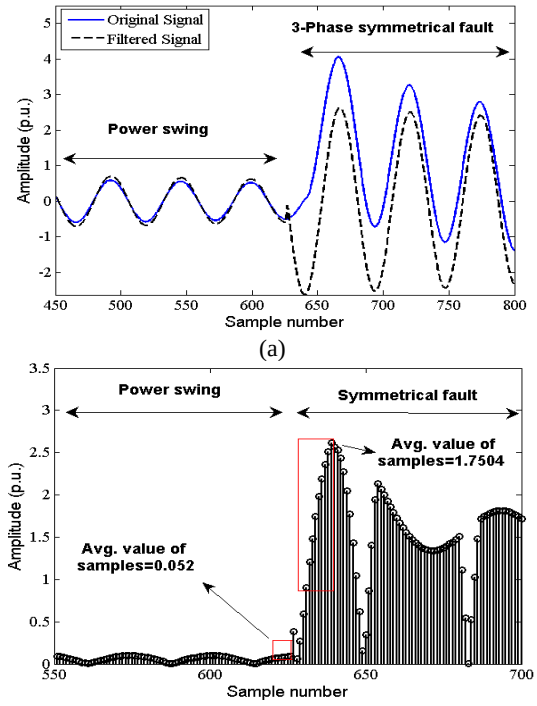

Fig. 8 Current waveforms following power swing and 3-phase symmetrical fault during Case 1. (a) Original and filtered signals. (b) Amplitude of the differential decaying DC component.

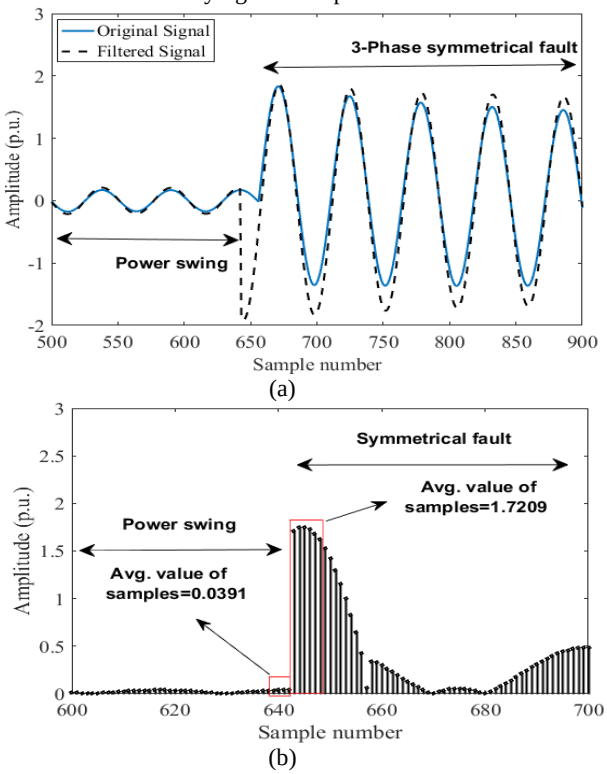

Fig. 9 Current waveforms following power swing and 3-phase symmetrical fault during Case 5. (a) Original and filtered signals. (b) Amplitude of the differential decaying DC component.

Consequently, discrimination of a symmetrical fault from a power swing in compensated power system is more complicated than in a simple power system due to the nonlinear performance of the series capacitor and its protection equipment. Therefore, the second IEEE benchmark model [32], as illustrated in Fig. 7(b) is used to verify the proposed technique on the series capacitor-compensated power system. As stated earlier, the exponentially decaying DC component is influenced by various factors in the power system. Consequently, various test scenarios are generated by varying degrees of compensation (i.e. the size of the series capacitor), fault resistance, fault inception time, and fault location.

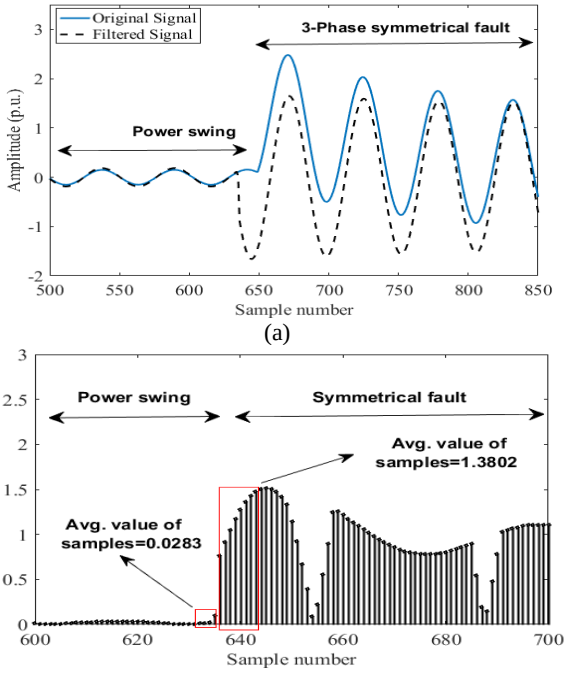

Fig. 10 Current waveforms following power swing and 3-phase symmetrical fault during Case 8. (a) Original and filtered signals. (b) Amplitude of the differential decaying DC component.

The series capacitor with various sizes is protected by metal-oxide-varistors (MOV) and is located at the ends of transmission line 1. MOV protection level is set at 2.5-times the nominal capacitor voltage. For creating the power swing condition in different cases, a temporary fault with various duration is applied after the beginning of the simulation. Furthermore, 3-phase symmetrical faults are applied at various time instants at different locations on line 2. These test scenarios and the associated results are presented in Table 3. According to Table 3, it can be clearly seen that there is a considerable value of AVDCS during the three-phase fault, while it has negligible value following the power swing condition. During case 16, a symmetrical fault is applied at the 1.005st second after the beginning of the simulation with inception

angle of 90°. In this case, fault resistance and fault location are considered 3 ohm and 40 km from the relay location, respectively at the 45% degree of compensation. Fig. 11(a) shows the original and filtered signals following the power swing and 3-phase symmetrical fault. Furthermore, Fig. 11(b) shows the magnitude of the differential decaying DC components (i.e. ΔI) during these power swing and 3-phase symmetrical fault.

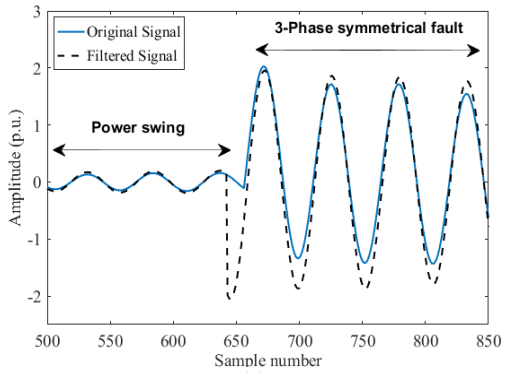

(a)

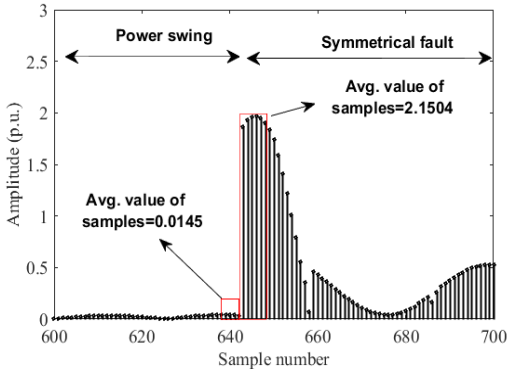

(b)

Fig. 11 Current waveforms following power swing and 3-phase symmetrical fault during Case 16. (a) Original and filtered signals. (b) Amplitude of the differential decaying DC component.

According to Fig. 11(b), it is evident that during power swing conditions, the amount of the AVDCS is negligible value, whereas it increases to a substantial amount after the fault inception.

In addition, to show the similarity in characteristics, Figs. 12 and 13 illustrate the original signal, filtered signals, and magnitude of the differential decaying DC component (i.e. ΔI) following a power swing and 3-phase symmetrical fault during cases 19 and 22. In these cases, the degrees of compensation are considered 60% and 70%, respectively. According to these Figs. 12 and 13, it can be seen that the amplitude of the differential decaying DC component has a unique behavior in different test scenarios, and its general pattern is not affected by the degrees of compensation, fault resistance, fault inception time, and fault location.

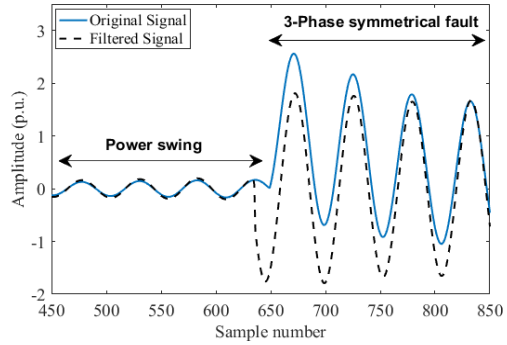

(a)

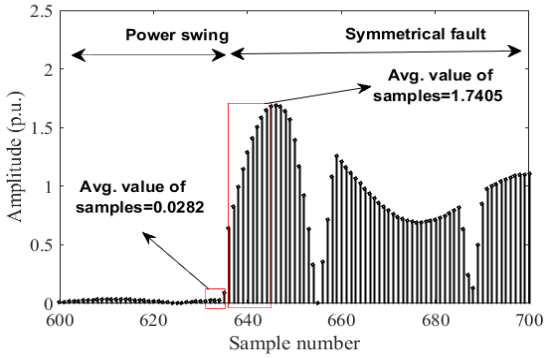

(b)

Fig. 12 Current waveforms following power swing and 3-phase symmetrical fault during Case 19. (a) Original and filtered signals. (b) Amplitude of the differential decaying DC component.

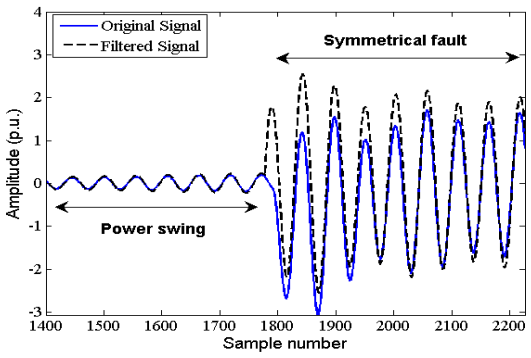

(a)

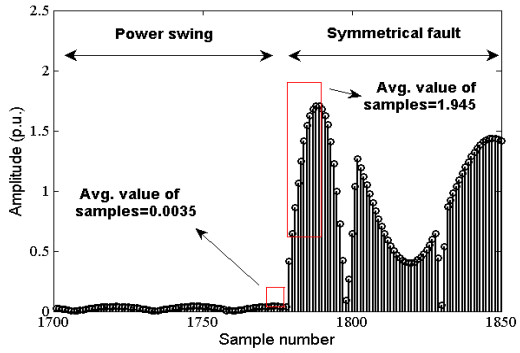

(b)

Fig. 13 Current waveforms following power swing and 3-phase symmetrical fault during Case 22 (a) Original and filtered signals. (b) Amplitude of the differential decaying DC component.

The results of this series capacitor-compensated power system indicate that the proposed technique is applicable to any kind of network and its realization is straightforward. It is worth highlighting that the application of the proposed technique is simple and it can be directly applied in any type of power system, even in the interconnected multi-generator power system. Another point worth highlighting is that the large value of the AVDCS during 3-phase symmetrical fault conditions can be utilized easily to ensure accurate discrimination between the power swing and 3-phase symmetrical fault. It should be noted that this diagnosis is instant and no intentional time delay is required after a quarter of one power cycle.

4.3 Faults with High Resistance

Detecting the faults with high resistance and differentiating them from power swing is more difficult than the low resistance fault detection. Generally speaking, in high resistance faults, the main signal used for diagnosis is less degraded, therefore the accuracy of the methods decreases in these types of faults. To check the performance of the proposed approach against faults with high resistance, the selected cases illustrated in Tables 4 and 5 have been considered.

Table 4 Different cases for studying the performance of the suggested technique against faults with high resistance at 50 km, fault inception=1.04 s, and with inception angles of 0 degree.

Case	Fault Resistance (ohm)	Average of the differential current samples (ΔI) in quarter of one cycle (p.u.)	
		Symmetrical fault conditions	Power swing conditions
23	25	1.202	0.11
24	50	1.13	0.15
25	75	1.05	0.165
26	100	0.995	0.186

Table 5 Different cases for studying the performance of the suggested technique against faults with high resistance at 50 km, 55% degree of compensation, fault inception=1.04 s, and with inception angles of 0 degree.

Case	Fault Resistance (ohm)	Average of the differential current samples (ΔI) in quarter of one cycle (p.u.)	
		Symmetrical fault conditions	Power swing conditions
27	25	1.19	0.105
28	50	1.121	0.145
29	75	1.001	0.159
30	100	0.991	0.178

These test scenarios and the associated results are presented in Tables 4 and 5. According to Tables 4 and 5, it can be clearly seen that there is a high value of AVDCS during the three-phase fault, while it has a small value following the power swing condition. However, in these conditions, due to the high resistance, the amplitude of the decaying DC component is reduced compared to the case where the fault resistance is lower. For instance, Fig. 14 shows the original, filtered signals and the magnitude of the differential decaying DC component (i.e. ΔI) following a power swing and 3-phase symmetrical fault during case 22. On the other hand, to show the similarity in characteristics, Fig. 15 illustrates the original, filtered signal, and magnitude of the differential decaying DC component (i.e. ΔI) following a power swing and 3-phase symmetrical fault during case 26. In this case, the degree of compensation is considered 55%. As stated earlier and due to these figures, it can be clearly seen that during power swing conditions, the amount of the AVDCS is a small value, whereas it increases to a high value after the fault inception.

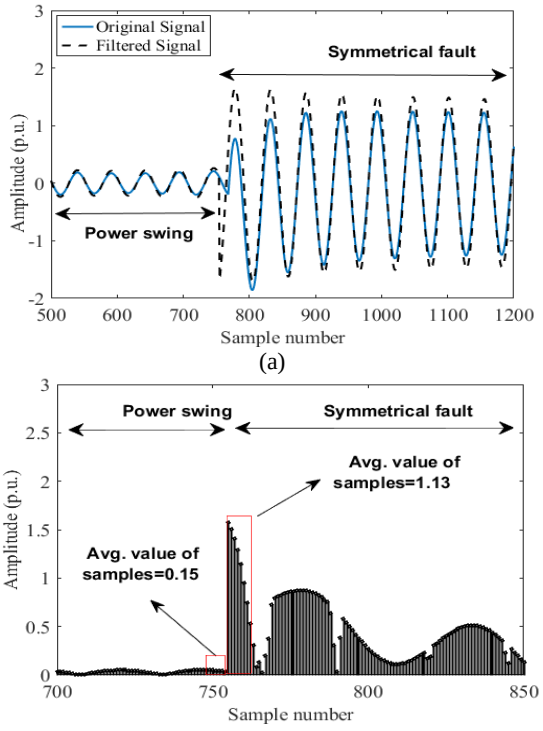

Fig. 14 Current waveforms following power swing and 3-phase symmetrical fault during Case 24. (a) Original and filtered signals. (b) Amplitude of the differential decaying DC component.

5 Power Swings with Different Frequencies

In this section, the performance of the suggested technique is analyzed following power swings with different frequencies. Therefore, several symmetrical 3-phase faults are considered during various power swing conditions. To produce the

power swings with various frequencies, the generator frequency is changed in the range of 1-6 Hz, while the infinite bus frequency is kept constant at 60 Hz [12]. It should be noted that the stable power swings have a low frequency, however, as soon as the network becomes unstable, these frequencies begin to increase [12]. Fig. 16(a) shows the original and filtered signals following the power swings with various frequencies.

Furthermore, Fig. 16(b) shows the magnitude of the differential decaying DC component (i.e. ΔI) during these conditions. According to this figure, as it should be expected during power swings with various frequencies, the average value of the differential current samples is negligible. In other words, the proposed technique is independent of the swing frequency.

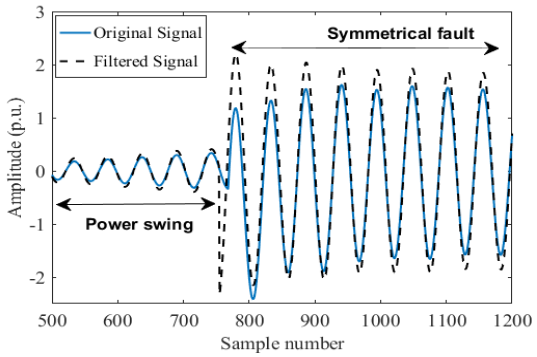

(a)

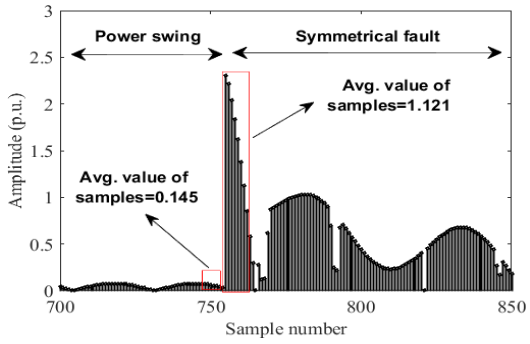

(b)

Fig. 15 Current waveforms following power swing and 3-phase symmetrical fault during Case 28. (a) Original and filtered signals. (b) Amplitude of the differential decaying DC component.

6 Comparative Analysis

As stated before, discrimination of a symmetrical 3-phase fault from a stable power swing is a great challenge for the accurate and safe operation of the distance relays. In other words, discrimination of these conditions with a fast and precise technique is very important for the operation of the power system. Consequently, for evaluation, a comparison is made between the proposed technique and some existing methods, and the results are presented in Table 6. The proposed technique needs that the digital MIMIC filter to be carried out on the current waveform. This unknown current waveform is measured in real-time, and as shown in Table 6, the proposed technique is very fast and is able to detect a symmetrical fault from a power swing in less than a quarter of one power cycle.

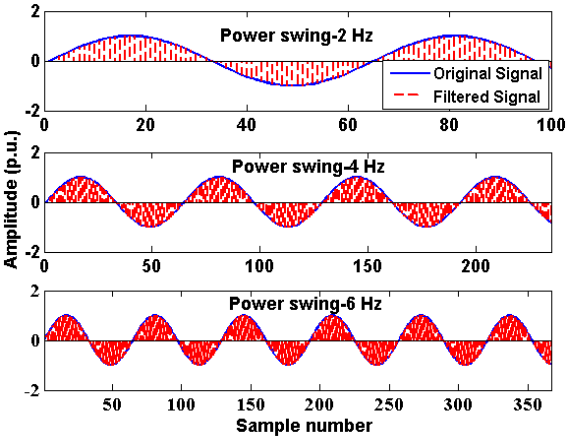

(a)

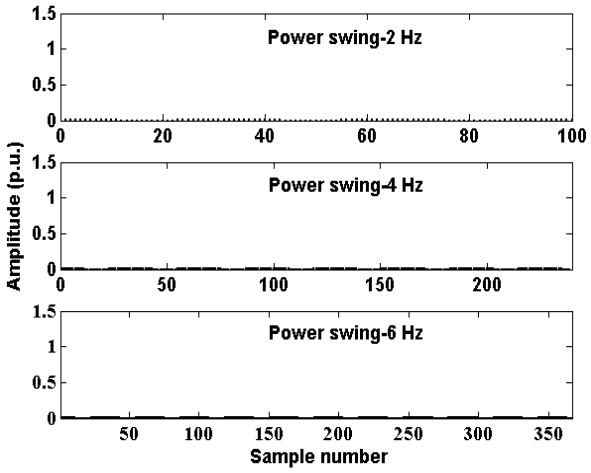

(b)

Fig. 16 Power swings with different frequencies. (a) Original and filtered signals. (b) Amplitude of the differential decaying DC component (i.e. difference between filtered and genuine samples of current).

The proposed technique does not need to accurately calculate the time constant of the DC component and is based only on the presence of the DC component. Therefore, the calculation burden in the method is reduced and the speed is increased. On the other hand, it is noteworthy that speed and accuracy together are important in discriminating a symmetrical 3-phase fault from a stable power swing. With high speed and accuracy in discrimination, the stresses on the power system are greatly reduced.

Table 6 Comparisons between the proposed technique and some existing methods for 60 Hz nominal frequency.

Method presented in	Requirement of signals	Detection time (ms)	Discrimination accuracy
[12]	FFT on 3-phase active power	16.67 (one cycle)	Not reported
[15]	Prony method on 3-phase current	5.66 (0.34 cycle)	Not reported
[24]	3V+3I at sending end	1.9	100%
[36]	3I at sending end	Not reported	97.5%
[37]	3I at sending end	16.67 (one cycle)	99%
[38]	3V and its harmonics at sending end	8.33	95%
Proposed	MIMIC filter on 3-phase current	4.17 (0.25 cycle)	100%

7 Conclusion

This paper introduces a new technique to discriminate a symmetrical 3-phase fault from a stable power swing based on the differential current. This differential current is computed from the difference between the filtered and genuine samples of the current waveform. In other words, the proposed technique uses the presence of the exponentially decaying DC component in the current waveform as a sign of the occurrence of a symmetrical fault, and this presence is detected by using a digital MIMIC filter. If there is no symmetrical fault in the power system, the difference between the filtered and genuine values of the current is found to be insignificant, else the difference is considerable. It is noteworthy that a digital MIMIC filter can be used for different sampling rates and there is no limit to this. The satisfactory performance of the suggested technique has been verified by simulating various cases on a single-circuit line and a series capacitor-compensated power system. The results illustrate that the proposed technique has several advantages over the existing techniques. The first is that the introduced technique is able to discriminate between symmetrical 3-phase faults from power swings in different types of power networks. The second advantage is that the introduced technique is very fast and this speed greatly improves the performance of the distance relay. Furthermore, various parameters such as fault location, fault inception time, fault resistance, swing frequency, and degree of compensation do not affect the speed and accuracy of the proposed technique.

Intellectual Property

The authors confirm that they have given due consideration to the protection of intellectual property associated with this work and that there are no impediments to publication, including the timing to publication, with respect to intellectual property.

Funding

No funding was received for this work.

Credit Authorship Contribution Statement

H. Yaghobi: Idea & Conceptualization, Research & Investigation, Data Curation, Analysis, Funding Acquisition, Methodology, Project Administration , Software and Simulation, Supervision, Verification, Original Draft Preparation, Revise & Editing.

Declaration of Competing Interest

The authors hereby confirm that the submitted manuscript is an original work and has not been published so far, is not under consideration for publication by any other journal and will not be submitted to any other journal until the decision will be made by this journal. All authors have approved the manuscript and agree with its submission to "Iranian Journal of Electrical and Electronic Engineering".

References

[1] Power Syst. relay Committee, "Power swing and out-of-step considerations on transmission lines," *IEEE PSRC Working Group D6*, New York, 2005.

[2] M. J. Abbasi and H. Yaghobi, "Loss of excitation detection in doubly fed induction generator by voltage and reactive power rate", *Iranian Journal of Electrical and Electronic Engineering*, Vol. 12, No. 4, pp. 270–280, 2016.

[3] Noroozi, Y. Alinejad-Beromi, H. Yaghobi, "Fast approach to detect generator loss of excitation based on reactive power variation,"

IET Generation, Transmission & Distribution, Vol. 13, No. 4, pp. 453-460, 2019.

[4] K.Venkatanagaraju and M. Biswal, "A Time-Frequency based backup protection scheme for enhancing grid security against power system blackout," *International Journal of Electrical Power & Energy Systems*, Vol. 137, pp. 107780, 2022.

[5] S. M. Hashemi and M. Sanaye-Pasand, "Distance protection during asymmetrical power swings: challenges and solutions," *IEEE Transactions on Power Delivery*, Vol. 33, No. 6, pp. 2736-2745, 2018.

[6] H. Yaghobi *et al.*, "A novel flux-based method for synchronous generator loss of excitation protection," in *Proc. 25th Int. Power Syst. Conf.*, Tehran, Iran, 2010.

[7] B. Su *et l.*, "Fast detector of symmetrical fault during power swing for distance relay," in *In IEEE Power Engineering Society General Meeting*, pp. 1836-1841, 2005.

[8] A. Mechaoui and D. W. P. Thomas, "A new blocking principle with phase and earth fault detection during fast power swings for distance protection," *IEEE Transactions on Power Delivery*, Vol. 10, No. 3, pp. 1242-1248, 1995.

[9] A. Mechaoui and D. W. P. Thomas, "A new principle for high resistance earth fault detection during fast power swings for distance protection," *IEEE Transactions on Power Delivery*, Vol. 12, No. 4, pp. 1452-1457, 1997.

[10] X. Lin, Gao, and P. Liu, "A novel scheme to identify symmetrical faults occurring during power swings," *IEEE Transactions on Power Delivery*, Vol. 23, No. 1, pp. 73-78, 2008.

[11] H. Khorashadi-Zadeh, "Evaluation and performance comparison of power swing detection algorithms," in *IEEE Power Engineering Society General Meeting*, pp. 976-982, 2005.

[12] B. Mahamedi and J. G. Zhu, "A novel approach to detect symmetrical faults occurring during power swings by using frequency components of instantaneous three-phase active power," *IEEE Transactions on Power Delivery*, Vol. 27, No. 3, pp. 1368-1376, 2012.

[13] H. K. Karegar and B. Mohamedi, "A new method for fault detection during power swing in distance protection," *6th International Conference on ECTI-CON*, Thailand, pp. 230-233, 2009.

[14] Y. Guo, M. Kezunovic, and D. Chen, "Simplified algorithms for removal of the effect of exponentially decaying DC-offset on the Fourier algorithm," *IEEE Transactions on Power Delivery*, Vol. 18, No. 3, pp. 711-717, 2003.

[15] S. Lotfifard, J. Faiz, and M. Kezunovic, "Detection of symmetrical faults by distance relays during power swings," *IEEE Transactions on Power Delivery*, Vol. 25, No. 1, pp. 81-87, 2010.

[16] P. N. Gawande and S. S. Dambhare, "A novel unblocking function for distance relay to detect symmetrical faults during power swing," *IEEE Power and Energy Society General Meeting* (PESGM), Boston, USA, 2016.

[17] J. T. Rao, B.R. Bhalja, M. Andreev, and O. P. Malik, "Synchrophasor assisted power swing detection for wind integrated transmission network," *IEEE Transactions on Power Delivery*, Vol. 37, No. 3, pp. 1952-1962, 2022.

[18] Z. Moravej, R. Ansari, and A. Jodaei, "Improvement of fault detection during power swing in series compensated line by using a Taylor series," *Computational Intelligence in Electrical Engineering*, Vol. 12, No. 2, pp. 65-76, 2021.

[19] I. G. Tekdemir and B. Alboyaci, "A novel approach for improvement of power swing blocking & deblocking functions in distance relays," *IEEE Transactions on Power Delivery*, Vol. 32, No. 4, pp. 1986-1994, 2017.

[20] T. R. Juttu, and B. R. Bhalja, "A new phase angle of superimposed positive sequence current-based discrimination scheme for prevention of maloperation of distance relay during severe stressed conditions," *IEEE System Journal*, Vol. 14, No. 3, pp. 3705-3716, 2020.

[21] H. Paula, C. S. Pereira, A. D. Conti, A.P. Morais, E.G. Silveira and J.S. Andrade, "Rotating negative-sequence phasors for blocking and unblocking the distance protection during power swings," *Electric Power Systems Research*, Vol. 202, pp. 1-12, 2022.

[22] S. M. Brahma, "Distance relay with out-of-step blocking function using wavelet transform," *IEEE Transactions on Power Delivery*, Vol. 22, No. 3, pp. 1360-1366, 2007.

[23] H. K. Zadeh and Z. Li, "A novel power swing blocking scheme using adaptive neuro-fuzzy inference system," *Electric Power Systems Research*, Vol. 78, pp. 1138-1146, 2008.

[24] M. Daryalal and M. Sarlak, "Fast fault detection scheme for series compensated lines during power swing," *International Journal of Electrical Power & Energy Systems*, Vol. 92, pp. 230-244, 2017.

[25] S. R. Bhide, *Digital Power System Protection.* New Delhi: PHI Learning Pvt. Ltd., 2014.

[26] G. Benmouyal, "Removal of decaying dc in current waveforms using digital mimic filtering," *IEEE Transactions on Power Delivery*, Vol. 10, No. 2, pp. 621-630, 1995.

[27] M. Rajabi Nasab and H. Yaghobi, "A real-time out-of-step protection strategy based on instantaneous active power deviation," *IEEE*

Transactions on Power Delivery, Vol. 36, No. 6, pp. 3590-3600, 2021.

[28] H. Zare, H. Yaghobi, Y. Alinejad-Beromi, "Adaptive concept of controlled islanding in power systems for wide-area out-of-step prediction of synchronous generators based on adaptive tripping index," *IET Generation, Transmission & Distribution*, Vol. 12, No. 16, pp. 3829-3836, 2018.

[29] H. Yaghobi, "Fast predictive technique for reverse power detection in synchronous generator," *IET Electric Power Applications*, Vol. 12, No. 4, pp. 508-517, 2018.

[30] R. Abd Allah, "Primary time constant calculation of power system," *International Journal of Engineering and Innovative Technology (IJEIT)*, Vol. 4, No. 1, pp. 69-74, 2014.

[31] S. H. Ashrafi Niaki and H. Kazemi Karegar, "An analytic method for removal of decaying DC component from phasor estimates," *Iranian Journal of Electrical and Computer Engineering*, vol. 12, no. 1, pp. 33-40, 2013

[32] R. G. Farmer, "Second benchmark model for computer simulation of subsynchronous resonance IEEE subsynchronous resonance working group of the dynamic system performance subcommittee power system engineering committee." *IEEE Power Engineering Review*, Vol. 5, pp. 34-34, 1985.

[33] H. Yaghobi, K. Ansari, and H. Rajabi mashhadi, "Stator turn-to-turn fault detection of synchronous generator using total harmonic distortion (THD) analyzing of magnetic flux linkage", *Iranian Journal of Science and Technology. Transactions of Electrical Engineering*, Vol. 37, No. E2, pp. 161-182, 2013.

[34] S. Paudyal, G. Ramakrishna and M. S. Sachdev, "Application of equal area criterion conditions in the time domain for out-of-step protection," *IEEE Transactions on Power Delivery*, Vol. 25, No. 2, pp. 600-609, 2010.

[35] H. Zare, Y. Alinejad-Beromi, and H. Yaghobi, "Intelligent prediction of out-of-step condition on synchronous generators because of transient instability crisis," *International Transactions on Electrical Energy Systems*, Vol. 29, No.1, pp.1-21, 2019.

[36] N. G. Chothani, B. R. Bhalja, and U. B. Parikh, "New support vector machine-based digital relaying scheme for discrimination between power swing and fault," *IET Generation, Transmission & Distribution*, Vol. 8, No. 1, pp. 17-25, 2014.

[37] R. Dubey, S. R. Samantaray, B. K. Panigrahi, and V. G. Venkoparao, "Phase-space-based symmetrical fault detection during power swing," *IET Generation, Transmission & Distribution*, Vol. 10, No. 8, pp. 1947-1956, 2016.

[38] E. Koley, S. K. Shukla, S. Ghosh, and D. K. Mohanta, "Protection scheme for power transmission lines based on SVM and ANN considering the presence of non-linear loads," *IET Generation, Transmission & Distribution*, Vol. 11, No. 9, pp. 2333-2341, 2017.

H. Yaghobi was born in Sari, Iran on 1978. He received the B.Sc. degree in electrical engineering from the K. N. Toosi University of Technology, Tehran, Iran, in 2000, the M.Sc. degree in electrical engineering from Ferdowsi University, Mashhad, Iran, in 2002, and the Ph.D. degree in electric machinery from the Department of Electrical Engineering, Ferdowsi University, Mashhad, Iran, in 2011. He is currently an Associate Professor with Semnan University, Semnan, Iran. His research interests include modeling and fault diagnosis, and design and protection of electrical machines.